

1. Introduction

Dissolved ammonia, ferrous iron and manganese exist widely in groundwater, especially in Northeast China (Qin et al., 2009; Cheng, 2016; Hasan et al., 2015). The presence of ammonia in drinking water treatment could affect the chlorination process (Cheng et al., 2017). Since ammonia would react with chlorine to form disinfection by-products (Richardson and Postigo, 2012; Du et al., 2017), which could produce deteriorate taste and odor of water (Cheng et al., 2016), reduce disinfection efficiency (Hasan et al., 2014), and damage human nervous system. In addition, ammonia can interfere with the manganese biofiltration process by consuming excessive oxygen during nitrification, resulted in mouldy and earthy tasting water (Hasan et al., 2014). The presence of iron and manganese can result in aesthetic and operational problems, such as giving water an undesirable color and odor, staining on laundry and accumulating in water distribution networks (Zeng et al., 2015). Therefore, the presence of ammonia, iron and manganese in drinking water should be avoided and the maximum contaminant levels (MCLs) for ammonia of 0.5 mg/L, total iron of 0.3 mg/L and manganese of 0.1 mg/L have been established in China (GB 5749-2006).

Chemical methods could be used to oxidize ammonia, iron and manganese, but it may produce potential hazardous by-products. Besides, it may also introduce other pollutants into the produced water (Cai et al., 2015). Thus, in the current circumstances, biological removal of ammonia, iron and manganese were emerged, and gradually replaced the conventional chemical treatments (Tekerekopoulou et al., 2013). As demonstrated, simultaneous removal of ammonia, iron and manganese could be accomplished in biological systems (Han et al., 2013; Hasan et al., 2012), where iron and manganese removal through biological oxidation could be achieved by iron oxidizing bacteria (IOB) and manganese oxidizing bacteria (MnOB), respectively. Meanwhile, several groups of bacteria have been confirmed as IOB (*Gallionella*, *Leptothrix*, *Bacillus* and *Leptothrix discophora* (Yang et al., 2014; Li et al., 2013)) and MnOB (*Leptothrix*, *Gallionella*, *Pseudomonas*, *Siderocapsa*, *Crenothrix*, *Hyphomicrobium* and *Metalloaenium* (Hasan et al., 2012; Tang et al., 2016; Mckee et al., 2016; Granger et al., 2014)). Biological ammonia oxidation is carried out by two different consecutive microbial processes, nitrification and nitratification, thus ammonia removal through biological oxidation could be finished by ammonia oxidizing bacteria (AOB) and nitrite oxidizing bacteria (NOB). Currently, several groups of bacteria have been confirmed as AOB and NOB, such as *Nitrosomonas europaea*, *Nitrosomonas halophila*, *Nitrosomonas mobilis*, *Nitrospira*, *Comamonas* and *Acinetobacter* (Hasan et al., 2012; Li et al., 2013).

Recently, the distribution and genetic diversity of the microorganisms in the biofilter for ammonia, iron and manganese removal were investigated by some researchers (Hasan et al., 2012; Li et al., 2013), however, the microbial community was studied only in steady phase or one operational condition. There were few reports regarding to the microbial community in different conditions and the relationship between the operational conditions and the microbial community in the biofilter. In addition, synthetic drinking water source with model chemicals, which was used in most reports, is definitely different from the real water resources; therefore, the microbial community in biological removal process from the two kinds of waters should be also different.

In this study, a pilot-scale biofilter was established for the simultaneous removal of ammonia, iron and manganese using anthracite and manganese sand as the media. Compared with other studies, real feed groundwater was selected to carry out this experiment. Approximately 112 d long-term operation was evaluated with respect to ammonia, iron and manganese removal, and

the microbial community structures from different depths of filter layer in different phases of the start-up process were analyzed and compared using 454 HTP. The main objectives of this study were to gain a deep insight into bacterial diversity in the biofilter, and the relationship between the microbial community and the removal efficiencies of ammonia, iron and manganese during the start-up process.

2. Materials and methods

2.1. Description of biofilter system

A pilot-scale biofilter system was developed in a groundwater treatment plant (GWTP), which is located in Harbin city, P.R. China (Fig. 1). The biofilter consisted of a 147.19 L transparent rigid plexi-glass column with an inner diameter of 250 mm and a height of 3000 mm in which a height of 1500 mm was packed with support materials. Along the height of the column there were 20 water sampling ports at 100 mm intervals, and 3 media sampling ports at 0, 400 and 800 mm from media top to bottom. During the long-term running of the biofilter, it was backwashed according to the water head loss and effluent turbidity.

To avoid the redox reaction occurred between Fe^{2+} and Mn^{4+} after backwashing, two kinds of new support materials with different density were packed in the biofilter: the upper part of the media (300 mm) was columnar anthracite with a mean diameter of 1 mm and a height of 5 mm, and the lower part (1200 mm) was manganese sand with a mean diameter of 0.8–1 mm.

Real groundwater, which was extracted from the wells with a depth of 40–50 m, in Harbin city, P.R. China, was used throughout this experiment. The concentration of total iron, manganese and ammonia in raw groundwater was about 8–13, 0.9–1.3 and 0.9–1.4 mg/L, respectively, and the temperature was about 8 °C (Table 1).

2.2. Start-up process

The raw groundwater was sprayed to the tank, and then pumped to the biofilter with a flow rate of 2 m/h (Fig. 1). It should be noted that backwashing water obtained from the GWTP was inoculated into the biofilter as inoculum and weak backwashing intensity ($5\text{--}7\text{ L}/(\text{s}\cdot\text{m}^2)$) was adopted to shorten the start-up period of the biofilter. When the concentration of ammonia, total iron and manganese in effluent decreased to 0.1, 0.3 and 0.1 mg/L, respectively, the flow rate was promoted to 3 m/h and then promoted to 4 and 6 m/h in the same way. And the backwashing intensity increased to $12\text{ L}/(\text{s}\cdot\text{m}^2)$, when the flow rate increased to 6 m/h. It was important to note that the concentration of ammonia, total iron and manganese was measured from the 6th day.

2.3. Sampling and analytical procedure

Water samples from the inlet and outlet were performed every day, and water samples along the height of the filter bed were performed twice a week. Ammonia, total iron and manganese in the water samples were measured by photometric method, according to standard methods for water and wastewater examination (Method NOs.: 4500-NH₃.B&C, 3500-Fe.B and 3500-Mn.B, respectively) (Li et al., 2013). The pH, dissolved oxygen (DO) and oxidation reduction potential (ORP) measurements were measured using a pH meter (pH 315i-WTW), a DO meter (Oxi 315i-WTW) and a ORP meter (pH 315i-WTW), respectively. The filter media (anthracite or manganese sands) were collected at three depths of the filter bed (0, 400 and 800 mm), and stored at $-80\text{ }^{\circ}\text{C}$ for further analysis. In addition, scanning electron microscopy (SEM, JSM-

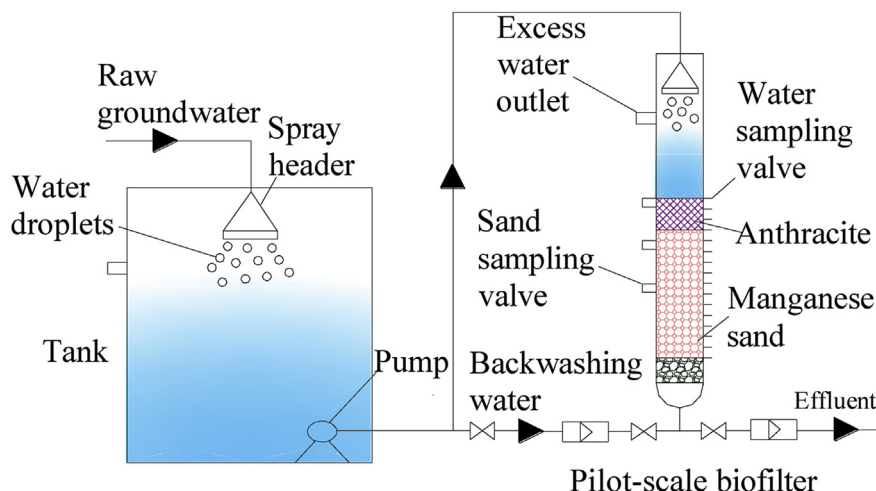


Fig. 1. Schematic drawing of the pilot-scale biofilter system.

Table 1
Physicochemical characteristics of the raw groundwater.

Properties	Value	Properties	Value
Temperature	~7.8 °C	NO ₂ ⁻	~0.002 mg/L
pH	~7.0	NH ₄ ⁺	~1.2 mg/L
Total Fe	~10 mg/L	COD _{Mn}	~1.8mgO ₂ /L
Mn	~1.1 mg/L	Color	18
Total As	<0.002 mg/L	DO	~0.2 mg/L
SO ₄ ²⁻	~5 mg/L	Alkalinity	220.0 mg CaCO ₃ /L
F ⁻	~0.5 mg/L	Turbidity	~1.5NTU
Cl ⁻	~2 mg/L	Total hardness	150–180 mg CaCO ₃ /L
NO ₃ ⁻	~0.04 mg/L		

6480LV) analysis was used to observe the morphology of the microorganisms in matured filter media from the biofilter, according to previous studies (Tang et al., 2016).

2.4. Microbial diversity analysis

2.4.1. DNA extraction and polymerase chain reaction (PCR) amplification

For a full understanding of the microbial community structure evolution resulting from different phases of the start-up process, media samples from three depths of the filter layer (0 mm, 400 mm and 800 mm) were analyzed by 454 HTP at days 25 (A1, A2 and A3), 69 (B1, B2 and B3) and 97 (C1, C2 and C3). DNA was extracted from the media samples (~0.5 g) taken from the biofilter using Powersoil DNA Isolation Kit (MoBio Laboratories Inc, USA) according to the manufacturer's instructions. The quality of the DNA were examined by 1% (w/v) agarose gel electrophoresis and the concentration was measured with a UV–Vis spectrophotometer (NanoDrop 2000, USA).

The V3–V4 region of the 16S rRNA gene was amplified using bacterial primers 515F (5'- GTG CCA GCM GCC GCG GTA A-3') and 806R (5'- GGA CTA CHV GGG TWT CTA AT-3'), with the reverse primer containing a 6 bp barcode used to tag each sample. PCR amplifications were carried out for each sample using 50 µL reaction mixtures, containing 5 µL of 10 × PCR buffer, 15 ng of template DNA, 1 µM of each primer, 0.6 mM of each dNTP, and 2 U FastPfu polymerase (TransGen, China). The PCR conditions involved an initial denaturation step at 94 °C for 3 min, followed by 29 cycles of 94 °C for 40 s, 56 °C for 1 min, and 72 °C for 1 min and ended with an extension step of 72 °C for 10 min in a GeneAmp 9700 thermocycler (ABI, USA). The amplicons were electrophoresed on a 2%

(w/v) agarose gel, and recovered using an AxyPrep DNA Gel Extraction Kit (AXYGEN, China).

2.4.2. 454 high-throughput 16S rRNA gene pyrosequencing

30 ng of DNA in each purified PCR product was taken for the equivalent mixture, and then the mixed DNA sample was electrophoresed in 1.5% (w/v) agarose gel and recovered by gel extraction kit (TransGen, China), finally sequencing of the mixed DNA sample was carried out on a Roche 454 GS FLX DNA sequencer (W.M. Keck Center, USA) according to standard protocols (Margulies et al., 2005). Raw pyrosequencing data of this study have been deposited to the NCBI Sequence Read Archive with accession No. SRP058656.

2.4.3. Biodiversity analysis and phylogenetic classification

Low quality reads (ambiguous nucleotides and quality value < 20) were removed from the raw sequence data as described in (Caporaso et al., 2011). The paired-end reads from each sample were overlapped to assembly V3–V4 tags of 16S rRNA gene using SeqPrep (<https://github.com/jstjohn/SeqPrep>), and then usearch6 was used to remove chimera sequences from the tags. Eventually, the numbers of high quality sequences were 15, 627 (A1), 5, 503 (A2), 31, 641 (A3), 28, 508 (B1), 8, 606 (B2), 11, 290 (B3), 11, 430 (C1), 11, 691 (C2) and 11, 123 (C3) with an average length of 291 bp.

The effective sequences were clustered into operational taxonomic units (OTUs) at 97% sequence identity using cd-hit embedded in Qiime (Caporaso et al., 2010), and then a representative sequence was picked for each OTU by selecting the most abundant sequence in that OTU. These representative sequences were assigned to taxonomic classifications by RDP Classifier with a confidence threshold of 70% (Wang et al., 2007; Chu et al., 2015). Furthermore, the alpha diversity including species richness estimator of Chao1, Shannon diversity index and diversity coverage were calculated in MOTHUR for each sample. Cluster analysis based on the Bray–Curtis similarity index was also carried out using PAST (<http://folk.uio.no/ohammer/past/>).

3. Results and discussion

3.1. Overall performance of the biofilter and SEM analysis

An excellent performance for iron removal was achieved, and total iron in effluent was all below 0.3 mg/L except the 33rd d (Fig. 2a). The removal rate of ammonia was only about 20% from

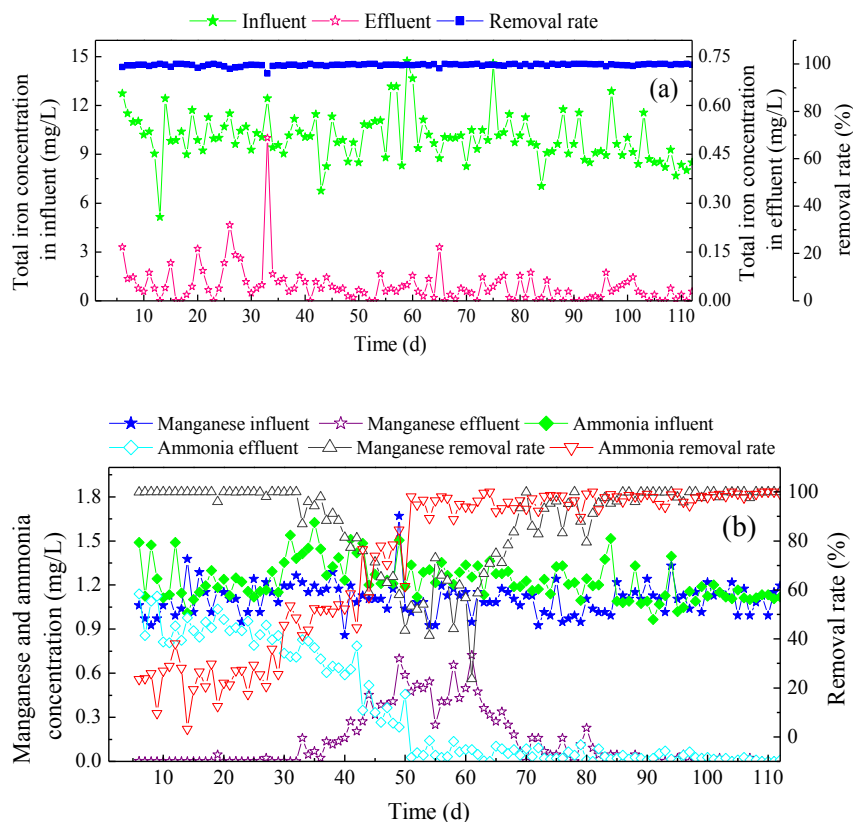


Fig. 2. Performance of biofilter with respect to simultaneous removal of iron (a), manganese and ammonia (b) in the start-up process.

the 6th to 29th d (Fig. 2b) and then quickly increased to 98.04% in the 51st d; during this time (the 30th to 51st d) nitrite was accumulated in the biofilter, because the rate of nitrosation is faster than that of nitrification, and the highest concentration of nitrite in effluent was 0.26 mg/L in the 43rd d (Fig. S1). Finally, ammonia in effluent was all lower than 0.15 mg/L since the 52nd d, and nitrate in effluent was about 0.8 mg/L, which was obviously lower than the MCL for nitrate of 10 mg/L in China (GB 5749-2006), while nitrite was not detected.

In the biofilter, manganese was removed in two ways: adsorbed by manganese sand which had a high ability to adsorb manganese, or oxidized by MnOB. Manganese in effluent was below 0.1 mg/L from the 6th to 32nd d (Fig. 2b), because it was adsorbed by manganese sand. And then manganese gradually increased to 0.72 mg/L in the 61st day, since manganese bed was getting saturated, while the MnOB oxidation was weak. Finally, manganese quickly decreased to 0.0012 mg/L in 70th d with MnOB accumulated in the filter media, and manganese was removed by MnOB oxidation. When the flow rate of the biofilter increased to 3, 4 and 6 m/h in the 71st, 76th and 79th d, respectively, the concentration of iron and ammonia was remained below the MCLs, while manganese was below the MCLs until 81st d, meaning that the biofilter was started successfully and the start-up period of the biofilter was 81 d. In steady phase, the efficiency of the biofilter indicated an excellent performance for ammonia, iron and manganese removal, and the corresponding removal efficiencies were 98.0%, 99.8% and 98.7%, respectively.

In the start-up process, iron was mainly removed at 0.4 m of the filter bed, and the corresponding removal efficiency was 98.80%, 98.89% and 95.48% in the 25th, 69th and 97th d, respectively (Fig. 3a). In the 25th d, manganese was mainly removed by

manganese sand adsorption, and the removal rate was 96.13% at 1.2 m; while manganese was mainly removed by MnOB oxidation in the 69th d, and the removal rate was 93.51% at 1.5 m. Manganese was mainly removed at 0.8 m in the 97th d, and the corresponding removal efficiency was 95.90% (Fig. 3b). And the removal rate of ammonia was gradually improved from 29.72% (25 d) to 93.95% (69 d) and 97.66% (97 d) with AOB and NOB accumulated in the biofilter; in steady phase, ammonia was mainly removed at 0.4 m, and the corresponding removal efficiency was 90.82% (Fig. 3c).

In order to verify bacteria existence and growth in the biofilter, SEM images of the mature media were observed. The micrograph illustrated that abundant microorganisms appeared in the mature media, and the surfaces of these bacteria were covered by large amounts of iron and manganese oxides, which evidenced the catalytic role of microorganisms in iron and manganese removal from groundwater (Fig. S2). A type of microorganisms with a very characteristic structure of twisted stalk may be the most common IOB (*Gallionella*), which was indigenous in groundwater and very common microorganisms in groundwater treatment plants for iron and manganese removal (Li et al., 2013). *Gallionella* is an obligative autotrophic bacterium and oxidizes ferrous iron to obtain energy for its growth (Arce-Rodríguez et al., 2017); it should be noted that this bacterium cannot oxidize manganese (Katsoyiannis and Zouboulis, 2004). Another type of microorganisms with a rod-shaped characteristic was also found in the biofilter, and this bacterium may be *bacillus*, which is an aerobic, endospore-forming, rod-shaped bacterium commonly found in soil, water sources and in association with plants (Kunst et al., 1995), and has the ability to catalyze manganese oxidation (Yang et al., 2014).

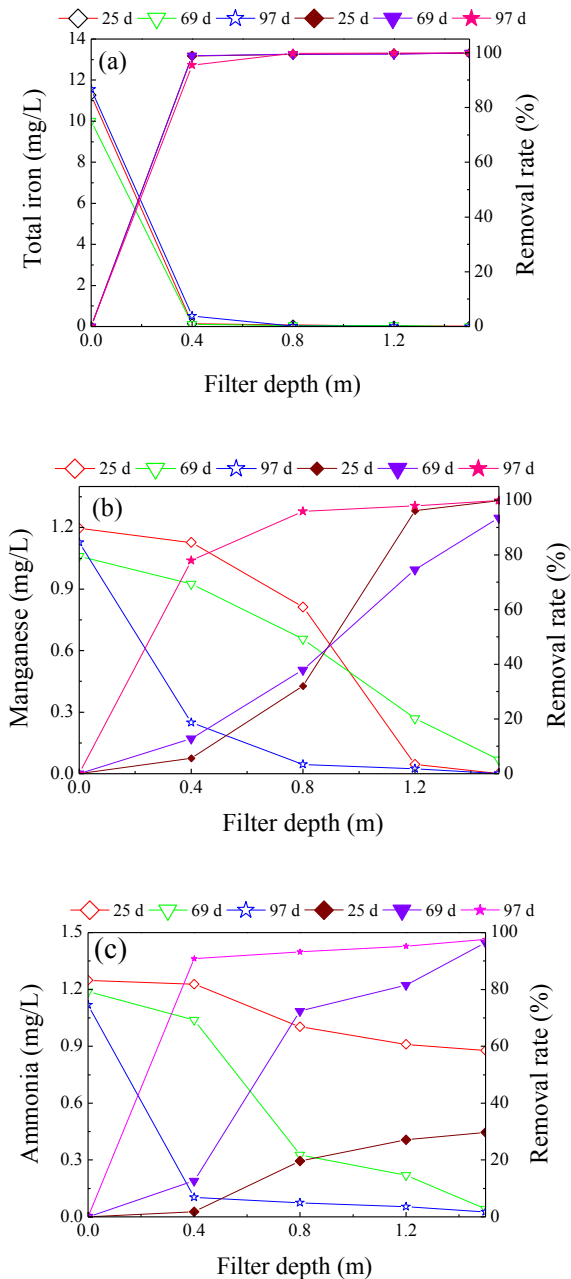


Fig. 3. Iron (a), manganese (b) and ammonia (c) removal profiles and removal efficiency along the height of biofilter in the start-up process.

3.2. Richness and diversity of bacteria phylotypes

Nine 16S rRNA gene libraries were constructed from pyrosequencing of A1, A2, A3, B1, B2, B3, C1, C2 and C3 communities with 15627, 5503, 31641, 28508, 8606, 11290, 11430, 11691 and 11123 high quality sequence tags (average length of 291 bp), respectively. By performing the alignment at a uniform length of 291 bp, 1107 (A1), 624 (A2), 1631 (A3), 1536 (B1), 907 (B2), 1290 (B3), 1021 (C1), 1118 (C2) and 1150 (C3) OTUs were clustered at a 3% distance (Table 2). The total number of OTUs estimated by Chao1 estimator were 2161 (A1), 1575 (A2), 2264 (A3), 2417 (B1), 1843 (B2), 2361 (B3), 1929 (C1), 2554 (C2) and 2079 (C3) with infinite sampling, indicating that C2 had the greatest richness, while A2 had the lowest richness. These results suggested that pyrosequencing

revealed bacterial communities were obviously different along the depths of the biofilter layer in different phases of the start-up process. The Shannon diversity index provides not only the simple species richness (i.e., the number of species present) but also how the abundance of each species is distributed (the evenness of the species) among all the species in the community. B3 had the highest diversity (Shannon = 7.73) among the nine communities, while A2 had the lowest diversity (Shannon = 6.74), and the Shannon diversity indexes of the others were all above 7 except A1.

3.3. Taxonomic complexity of the bacterial community

To identify the phylogenetic diversity of bacterial communities in A1, A2, A3, B1, B2, B3, C1, C2 and C3, qualified reads were assigned to know phyla, classes and genera. The nine communities showed an extremely high diversity, reflected in the fact that 31 (A1), 28 (A2), 41 (A3), 29 (B1), 26 (B2), 33 (B3), 28 (C1), 27 (C2) and 26 (C3) identified bacterial phyla were detected (Fig. 4), and in total, 42 identified bacterial phyla and 3 identified archaea phyla were observed. Even so, 1.41% (A1), 1.56% (A2), 1.25% (A3), 1.63% (B1), 1.86% (B2), 2.45% (B3), 1.31% (C1), 1.18% (C2) and 2.91% (C3) of the total reads in each sample were not classified at the phylum level, indicating that these bacteria are unknown. *Proteobacteria* was the dominant bacterial phyla, accounted for 74.43% (A1), 78.63% (A2), 74.92% (A3), 77.36% (B1), 74.95% (B2), 66.93% (B3), 76.32% (C1), 78.20% (C2) and 67.99% (C3) of the total reads, and existed widely in biofilters for the treatment of groundwater containing iron and manganese (Katsoyiannis and Zouboulis, 2004). *Verrucomicrobia* was accumulated in 0.8 m of the filter bed in the start-up process, and the abundance increased from 0.28% (A3) to 2.35% (B3) and 4.39% (C3); while it was lower than 0.8% in the other communities. *Nitrospirae* which involved in nitrification (Lu et al., 2012), existed in all nine communities, and was highest in abundance in C3 (1.26%).

The class level identification of the bacterial communities in the nine samples was illustrated in Fig. 5. Pyrosequencing detected 100 bacterial classes and 7 archaea classes in all nine communities, and 61, 53, 90, 66, 59, 72, 62, 58 and 63 bacterial classes were detected in A1, A2, A3, B1, B2, B3, C1, C2 and C3, respectively. *Gammaproteobacteria* and *Betaproteobacteria* were the most dominant bacterial community in the nine communities, and the sum of the two classes accounted for 69.45% (A1), 73.39% (A2), 67.03% (A3), 64.28% (B1), 61.70% (B2), 56.64% (B3), 66.61% (C1), 68.05% (C2) and 59.37% (C3) of the total reads. The abundance of *Flavobacteriia Alphaproteobacteria*, *Deltaproteobacteria*, and *Actinobacteria* was relatively

Table 2

Richness and diversity estimators of the bacteria phylotypes in the biofilter.

Sample ID	a = 0.03			
	OTU	Chao1 ^a	Shannon ^b	Coverage ^c
A1	1107	2161	6.76	0.95
A2	624	1575	6.74	0.91
A3	1631	2264	7.04	0.98
B1	1536	2417	7.27	0.97
B2	907	1843	7.45	0.94
B3	1290	2361	7.73	0.93
C1	1021	1929	7.05	0.94
C2	1118	2554	7.15	0.93
C3	1150	2079	7.16	0.94

^a Chao1 richness estimator: the total number of OTUs estimated by infinite sampling. A higher number indicates higher richness.

^b Shannon diversity index: an index to characterize species diversity. A higher value represents more diversity.

^c Good's coverage: estimated probability that the next read will belong to an OTU that has already been found.

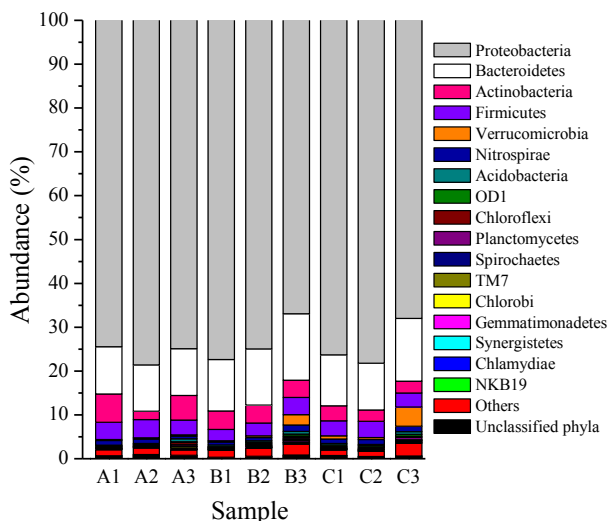


Fig. 4. Taxonomic classification of pyrosequences from bacterial communities of the nine samples at the phylum levels. Phyla with relative low abundance in all nine libraries were classified as "others".

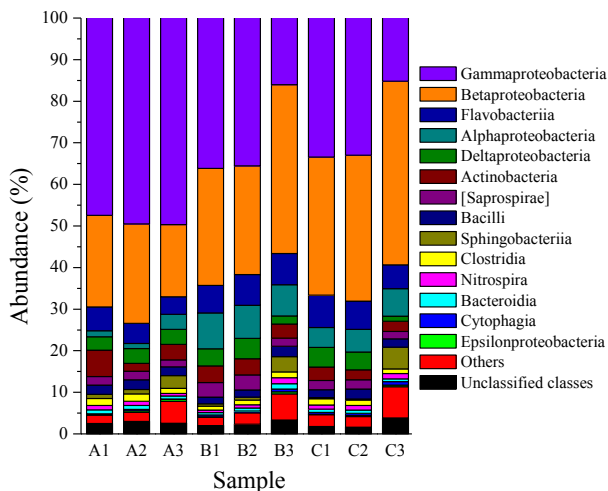


Fig. 5. Taxonomic classification of pyrosequences from bacterial communities of the nine samples at the class levels. Classes with relative low abundance in all nine libraries were classified as "others".

high in the nine communities.

At the genus level, 7.30% (A1), 5.92% (A2), 9.15% (A3), 7.15% (B1), 7.62% (B2), 12.30% (B3), 6.75% (C1), 6.21% (C2) and 10.51% (C3) of the total reads in each sample were not classified (Fig. 6). At the beginning of the start-up process (25 d), the dominant population in A1 (34.77%), A2 (37.44%) and A3 (29.37%) was *Crenothrix*, which not only can oxidize iron, but also manganese. The relative abundance genera were *Methylotenera* (12.45%, 14.15% and 6.19%) and *Methylomonas* (9.58%, 9.34% and 14.85%). IOB were found in the biofilter, such as *Bacillus*, *Leptospirillum*, *Crenothrix*, *Pseudomonas* and *Gallionella*, and MnOB were also found, such as *Bacillus*, *Arthrobacter*, *Crenothrix*, *Pseudomonas*, *Gallionella* and *Hyphomicrobium*. The appearance of AOB (*Nitrosomonas*, *Nitrosovibrio* and *Nitrosococcus*) and NOB (*Nitrospira*) demonstrated that nitrification and nitratification occurred in the biofilter to remove ammonia and nitrite, respectively (Lu et al., 2012; Li et al., 2017). Furthermore, there were many other kinds of genera in the biofilter, such as *Methylomonas* and *Methylotenera* may be methane oxidizing

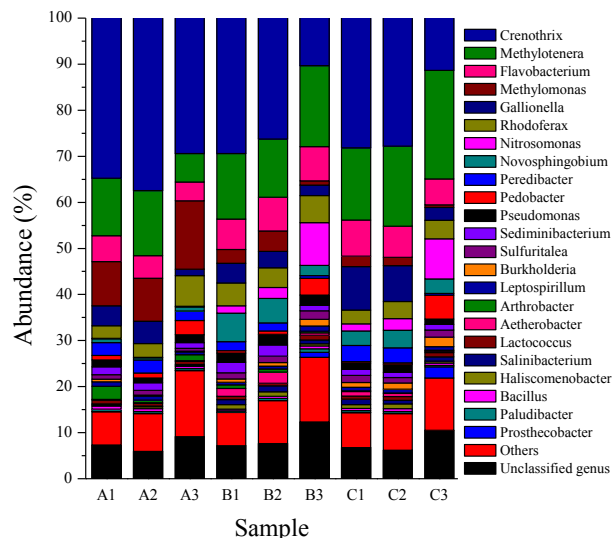


Fig. 6. Taxonomic classification of pyrosequences from bacterial communities of the nine samples at the genus levels. Genera with relative low abundance in all nine libraries were classified as "others".

bacteria, *Flavobacterium*, *Burkholderia*, *Novosphingobium* and *Paludibacter* may oxidize organic matter, and *Sulfuritalea* may be a sulfur oxidizer, since the composition of the real groundwater was complex.

Ferrous iron was oxidized by DO or IOB in the biofilter. At the beginning of the start-up period process (25 d), the high abundance of IOB and high efficiency of iron removal indicated that IOB were easily inoculated and then quickly accumulated in the biofilter, and the abundance of *Crenothrix*, *Gallionella*, *Leptospirillum* and *Bacillus* in A3 was obviously lower than that in A1 and A2, which agreed with the previous result that iron was mainly removed in 0–0.4 m of the filter bed. In the 25th day, manganese was mainly removed by manganese sand adsorption, meaning MnOB need more time to adapt the new environment and grow and multiply; ammonia was removed by AOB and NOB, but the abundance of AOB and NOB was relatively low, therefore the removal rate of ammonia was only 29.30% in this stage. Furthermore, the abundance of *Nitrosomonas* in A3 (0.14%) was obviously higher than that in A1 (0.098%) and A2 (0.089%), which was in accordance with that the removal quantity of ammonia in 0.8 m was obviously higher than that in 0 and 0.4 m. The abundance of the genera in A1 and A2 was not varied much, while the abundance of *Methylotenera* in A3 were much lower than those in A1 and A2; conversely, the abundance of *Methylomonas*, *Rhodoferrax* and *Pedobacter* was much higher than those in A1 and A2.

Most of IOB detected in the biofilter had the ability to oxidize manganese, such as *Crenothrix*, *Gallionella*, *Pseudomonas* and *Bacillus*. In the medium term of the start-up period process (69 d), *Crenothrix* (29.37%, 26.24% and 10.33%) which was IOB or MnOB, was the dominant genera in B1, B2 and B3; meanwhile, iron was completely removed, and manganese with a removal rate of 85.37% was mainly removed by MnOB. The abundance of *Crenothrix* and *Gallionella* in 69 d was obviously lower than those in 25 d in the same filter bed except *Gallionella* in B3. The reason was as followed: *Crenothrix* and *Gallionella* were continually accumulated in the biofilter, but the accumulating rates of them were slower than other bacteria, such as *Nitrosomonas*, *Flavobacterium* and *Methylotenera*. And the abundance of *Crenothrix* and *Gallionella* in B3 was obviously lower than those in B1 and B2, because the concentration of iron in influent was much higher than manganese, iron was

completely removed in 0.4 m of the filter bed, and only part of manganese was removed in 0.8 m. *Nitrosomonas* was accumulated in the biofilter in 69 d, and the abundance was 1.62% (B1), 2.37% (B2) and 9.27% (B1), which was obviously higher than that in 25 d (0.098%, 0.089% and 0.14%); correspondingly, the removal rate of ammonia was increased to 96.42% from 29.30%. And the abundance of *Nitrosomonas* in B3 was much higher than that in B1 and B2, agreed with that ammonia was mainly removed in 0.8 m of the filter bed.

In the steady phase of the start-up process (97 d), the dominant genera in C1, C2 and C3 were *Crenothrix* (28.18%, 27.82% and 11.33%) and *Methylotenera* (15.67%, 17.34% and 23.56%). And ammonia, iron and manganese were all mainly removed in 0–0.4 m of the filter bed. The abundance of *Crenothrix* and *Gallionella* decreased along the filter bed, according with iron decline along the filter bed. In 0.8 m, the removal rate of manganese in 97 d was much higher than that in 69 and 25 d, but the abundance of MnOB was not obviously increased in that filter bed. The reasons were as following: manganese was mainly removed in 0.4 m of the biofilter, other kinds of bacteria were accumulated in 0.8 m, and the oxidation efficiency of MnOB may much higher than other bacteria, such as IOB, AOB and NOB. The abundance of *Nitrosomonas* decreased in C3 but increased in C2 compared with that in 69 d, which agreed with that the main removal position of ammonia in the biofilter was transferred from 0.4–0.8 m in 69 d to 0–0.4 m in 97 d. In addition, the distribution of *Nitrosomonas* along the filter depth in 97 d was similar to that in 69 d. The abundance of *Prostheco bacter*, *Pedobacter*, and *Methylotenera* in C3 were much higher than those in C1 and C2, while *Peredibacter* and *Methylomonas* in C3 were much lower than those in C1 and C2. The abundance of *Methylotenera*, *Novosphingobium*, *Prostheco bacter* and *Burkholderia* in 0.8 m gradually increased from the 25–69 d and 97 d.

In the start-up process, the abundance of IOB was high, while the abundance of AOB and NOB increased with ammonia decreased in effluent, and biological manganese removal was gradually improved. IOB, MnOB, AOB and NOB were all existed in the nine communities, and the abundance of IOB and MnOB in 0.8 m of the filter bed was obviously lower than those in 0 and 0.4 m, while the abundance of AOB and NOB in 0.8 m was much higher than those in 0 and 0.4 m.

3.4. Composition of the archaea community

The numbers of reads of the archaea 16S rRNA gene accounted for 0.36% (A1), 0.49% (A2), 0.29% (A3), 0.19% (B1), 0.36% (B2), 0.43% (B3), 0.32% (C1), 0.33% (C2) and 0.29% (C3) of the total 16S rRNA genes. Pyrosequencing detected 3 archaea phyla-*Crenarchaeota*, *Euryarchaeota* and [*Parvarchaeota*], and 7 archaea classes-*MCG*, *Thaumarchaeota*, *DSEG*, *Methanobacteria*, *Methanomicrobia*, *Thermoplasmata* and [*Parvarchaeae*] in all nine communities (Fig. S3), and the dominant phylum and class were *Euryarchaeota* and *Thermoplasmata*, respectively, accounted for 100% (A1), 90.91% (A2), 86.59% (A3), 97.92% (B1), 100.00% (B2), 97.56% (B3), 100% (C1), 100% (C2) and 100.00% (C3); and 68.75% (A1), 54.55% (A2), 47.56% (A3), 60.42% (B1), 70.37% (B2), 56.10% (B3), 70.00% (C1), 78.12% (C2) and 57.14% (C3) of the total archaea 16S rRNA genes, respectively. The dominant genera in the nine communities were *Ferroplasma* (45.83%, 13.64%, 29.27%, 25.00%, 40.74%, 21.95%, 40.00%, 46.88%, and 32.14%) and *Thermogymnomonas* (22.92%, 40.91%, 18.29%, 35.42%, 29.63%, 34.15%, 30.00%, 31.25%, and 25.00%) (Fig. S4). Additionally, *Ferroplasma* was iron oxidizing archaea (IOA) (Rawlings, 2005), *Candidatus Nitrososphaera* was ammonia oxidizing archaea (AOA) (Oishi et al., 2012), *Nitrosopumilus* was possible related to denitrification (Li et al., 2014), and *Methanobacterium*, *Methanosaeta*, *Methanosarcina*, *Methanospirillum*, *Candidatus Methanoregula*,

Methanoculleus and *Methanobrevibacter* were possible related to methane oxidizing (Bharathi and Chellapandi, 2017; Rocheleau et al., 1999).

4. Conclusion

In the steady phase of the start-up process, ammonia, iron and manganese were removed at the upper part of the filter bed. AOB, NOB, AOA, IOB, IOA, MnOB which were related to ammonia, iron and manganese removal, and kinds of other bacteria which may be related to methane, hydrogen sulfide and organic matter removal, were found in the biofilter treating real groundwater. The spatial distribution of microbial populations along the depth of the biofilter revealed the stratification of the removal of ammonia, iron and manganese. The variation of spatial distribution of microbial populations in the biofilter revealed the increasing efficiencies of ammonia, iron and manganese removal during start-up process.

Acknowledgments

This work was supported by Fundamental Research Funds for the Central Universities (Izujbky-2015-137) and Scientific Research Foundation of CUIT (KYTZ201511).

Appendix A. Supplementary data

Supplementary data related to this article can be found at <http://dx.doi.org/10.1016/j.chemosphere.2017.05.075>.

References

- Arce-Rodríguez, A., Puente-Sánchez, F., Avendaño, R., Libby, E., Rojas, L., Cambroner, J.C., Pieper, D.H., Timmis, K.N., Chavarria, M., 2017. Pristine but metal-rich Río Suctio (Dirty River) is dominated by *Gallionella* and other iron-sulfur oxidizing microbes. *Extrem. Life Under Extreme Cond.* 21, 235–243.
- Bharathi, M., Chellapandi, P., 2017. Intergenomic evolution and metabolic cross-talk between rumen and thermophilic autotrophic methanogenic archaea. *Mol. Phylogenet. Evol.* 107, 293–304.
- Cai, Y.A., Li, D., Liang, Y.W., Luo, Y.H., Zeng, H.P., Zhang, J., 2015. Effective start-up biofiltration method for Fe, Mn, and ammonia removal and bacterial community analysis. *Bioresour. Technol.* 176, 149–155.
- Caporaso, J.G., Kuczynski, J., Stombaugh, J., Bittinger, K., Bushman, F.D., Costello, E.K., Fierer, N., Pena, A.G., Goodrich, J.K., Gordon, J.I., 2010. QIIME allows analysis of high-throughput community sequencing data. *Nat. Methods* 7, 335–336.
- Caporaso, J.G., Lauber, C.L., Walters, W.A., Berg-Lyons, D., Lozupone, C.A., Turnbaugh, P.J., Fierer, N., Knight, R., 2011. Global patterns of 16S rRNA diversity at a depth of millions of sequences per sample. *Proc. Natl. Acad. Sci. U.S.A.* 108, 4516–4522.
- Cheng, Q.F., 2016. Competitive mechanism of ammonia, iron and manganese for dissolved oxygen using pilot-scale biofilter at different dissolved oxygen concentrations. *Water Sci. Technol. Water Supply* 16, 766–774.
- Cheng, Q.F., Nengzi, L.C., Xu, D.Y., Guo, J.Y., Yu, J., 2016. Influence of nitrite on the removal of Mn(II) using pilot-scale biofilters. *J. Water Reuse Desalination*. <http://dx.doi.org/10.2166/wrd.2016.210>.
- Cheng, Q.F., Nengzi, L.C., Bao, L.L., Wang, Y.J., Yang, J.X., Zhang, J., 2017. Interactions between ammonia, iron and manganese removal using pilot-scale biofilters. *J. Water Supply Res. Technol. AQUA*. <http://dx.doi.org/10.2166/aqua.2017.089>.
- Chu, Z.R., Wang, K., Li, X.K., Zhu, M.T., Yang, L., Zhang, J., 2015. Microbial characterization of aggregates within a one-stage nitritation–anammox system using high-throughput amplicon sequencing. *Chem. Eng. J.* 262, 41–48.
- Du, X., Liu, G.Y., Qu, F.S., Li, K., Shao, S.L., Li, G.B., Liang, H., 2017. Removal of iron, manganese and ammonia from groundwater using a PAC-MBR system: the anti-pollution ability, microbial population and membrane fouling. *Desalination* 403, 97–106.
- Granger, H.C., Stoddart, A.K., Gagnon, G.A., 2014. Direct biofiltration for manganese removal from surface water. *J. Environ. Eng.* 140, 223–224.
- Han, M., Zhao, Z.W., Gao, W., Cui, F.Y., 2013. Study on the factors affecting simultaneous removal of ammonia and manganese by pilot-scale biological aerated filter (BAF) for drinking water pre-treatment. *Bioresour. Technol.* 145, 17–24.
- Hasan, H.A., Abdullah, S.R.S., Kofli, N.T., Kamarudin, S.K., 2012. Effective microbes for simultaneous bio-oxidation of ammonia and manganese in biological aerated filter system. *Bioresour. Technol.* 124, 355–363.
- Hasan, H.A., Abdullah, S.R.S., Kamarudin, S.K., Kofli, N.T., Anuar, N., 2014. Kinetic evaluation of simultaneous COD, ammonia and manganese removal from drinking water using a biological aerated filter system. *Sep. Purif. Technol.* 130,

- 56–64.
- Hasan, H.A., Abdullah, S.R.S., Kamarudin, S.K., Kofli, N.T., 2015. Effective curves of completing simultaneous ammonium and manganese removal in polluted water using a biological aerated filter. *J. Ind. Eng. Chem.* 30, 153–159.
- Katsoyiannis, I.A., Zouboulis, A.I., 2004. Biological treatment of Mn(II) and Fe(II) containing groundwater: kinetic considerations and product characterization. *Water Res.* 38, 1922–1932.
- Kunst, F., Vassarotti, A., Danchin, A., 1995. Organization of the European *Bacillus subtilis* genome sequencing project. *Microbiology* 389, 84–87.
- Li, X.K., Chu, Z.R., Liu, Y.J., Zhu, M.T., Yang, L., Zhang, J., 2013. Molecular characterization of microbial populations in full-scale biofilters treating iron, manganese and ammonia containing groundwater in Harbin, China. *Bioresour. Technol.* 147, 234–239.
- Li, P., Jiang, D., Li, B., Dai, X.Y., Wang, Y.H., Jiang, Z., Wang, Y.X., 2014. Comparative survey of bacterial and archaeal communities in high arsenic shallow aquifers using 454 pyrosequencing and traditional methods. *Ecotoxicology* 23, 1878–1889.
- Li, D., Stanford, B., Dickenson, E., Khunjar, W.O., Homme, C.L., Rosenfeldt, E.J., Sharp, J.O., 2017. Effect of advanced oxidation on N-nitrosodimethylamine (NDMA) formation and microbial ecology during pilot-scale biological activated carbon filtration. *Water Res.* 113, 160–170.
- Lu, L., Xing, D.F., Ren, N.Q., 2012. Pyrosequencing reveals highly diverse microbial communities in microbial electrolysis cells involved in enhanced H₂ production from waste activated sludge. *Water Res.* 46, 2425–2434.
- Margulies, M., Egholm, M., Altman, W.E., Attiya, S., Bader, J.S., Bembem, L.A., Berka, J., Braverman, M.S., Chen, Y.J., Chen, Z.T., Dewell, S.B., Du, L., Fierro, J.M., Gomes, X.V., Godwin, B.C., He, W., Helgesen, S., Ho, C.H., Irzyk, G.P., Jando, S.C., Alenquer, M.L.L., Jarvie, T.P., Jirage, K.B., Kim, J.B., Knight, J.R., Lanza, J.R., Leamon, J.H., Lefkowitz, S.M., Lei, M., Li, J., Lohman, K.L., Lu, H., Makhijani, V.B., McDade, K.E., McKenna, M.P., Myers, E.W., Nickerson, E., Nobile, J.R., Plant, R., Puc, B.P., Ronan, M.T., Roth, G.T., Sarkis, G.J., Simons, J.F., Simpson, J.W., Srinivasan, M., Tartaro, K.R., Tomasz, A., Vogt, K.A., Volkmer, G.A., Wang, S.H., Wang, Y., Weiner, M.P., Yu, P.G., Begley, R.F., Rothberg, J.M., 2005. Genome sequencing in micro fabricated high-density picolitre reactors. *Nature* 437, 376–380.
- McKee, K.P., Vance, C.C., Karthikeyan, R., 2016. Biological manganese oxidation by *Pseudomonas putida* in trickling filters. *J. Environ. Sci. Health Part A Toxic/Hazard. Subst. Environ. Eng.* 51, 523–535.
- Oishi, R., Tada, C., Asano, R., Yamamoto, N., Suyama, Y., Nakai, Y., 2012. Growth of ammonia-oxidizing archaea and bacteria in cattle manure compost under various temperatures and ammonia concentrations. *Microb. Ecol.* 63, 787–793.
- Qin, S.Y., Ma, F., Huang, P., Yang, J.X., 2009. Fe (II) and Mn (II) removal from drilled well water: a case study from a biological treatment unit in Harbin. *Desalination* 245, 183–193.
- Rawlings, D.E., 2005. Characteristics and adaptability of iron- and sulfur-oxidizing microorganisms used for the recovery of metals from minerals and their concentrates. *Microb. Cell Factories* 4.
- Richardson, S.D., Postigo, C., 2012. Drinking water disinfection by-products. In: *The Handbook of Environmental Chemistry Emerging Organic Contaminants and Human Health*, vol. 20. Springer, New York, NY, pp. 93–137. Chapter 4.
- Rocheleau, S., Greer, C.W., Lawrence, J.R., Cantin, C., Laramée, L., Guiot, S.R., 1999. Differentiation of *Methanosaeta concilii* and *Methanosarcina barkeri* in anaerobic mesophilic granular sludge by fluorescent in situ hybridization and confocal scanning laser microscopy. *Appl. Environ. Microbiol.* 65, 2222–2229.
- Tang, W.W., Gong, J.M., Wu, L.J., Li, Y.F., Zhang, M.T., Zeng, X.P., 2016. DGGE diversity of manganese mine samples and isolation of a *lysiniibacillus* sp. efficient in removal of high Mn (II) concentrations. *Chemosphere* 165, 277–283.
- Tekerlekopoulou, A.G., Pavlou, S., Vayenas, D.V., 2013. Removal of ammonium, iron and manganese from potable water in biofiltration units: a review. *J. Chem. Technol. Biotechnol.* 88, 751–773.
- Wang, Q., Garrity, G.M., Tiedje, J.M., Cole, J.R., 2007. Naive Bayesian classifier for rapid assignment of rRNA sequences into the new bacterial taxonomy. *Appl. Environ. Microbiol.* 73, 5261–5267.
- Yang, L., Li, X.K., Chu, Z.R., Ren, Y.H., Zhang, J., 2014. Distribution and genetic diversity of the microorganisms in the biofilter for the simultaneous removal of arsenic, iron and manganese from simulated groundwater. *Bioresour. Technol.* 156, 384–388.
- Zeng, X.P., Xia, J., Wang, Z.Z., Li, W.H., 2015. Removal of iron and manganese in steel industry drainage by biological activated carbon. *Desalination Water Treat.* 56, 2543–2550.

See discussions, stats, and author profiles for this publication at: <https://www.researchgate.net/publication/316910114>

Distribution and genetic diversity of microbial populations in the pilot-scale biofilter for simultaneous removal of ammonia, iron and manganese from real groundwater

Article in *Chemosphere* · May 2017

DOI: 10.1016/j.chemosphere.2017.05.075

CITATIONS

17

READS

26

8 authors, including:



[Yang Huang](#)

Chengdu University of Information Technology

17 PUBLICATIONS 122 CITATIONS

SEE PROFILE